Hydrogen isotope substitution on a water in oil micro-emulsion: quasi-elastic light scattering

Reprinted from The Journal of Physical Chemistry, 1995, 99.

Hydrogen Isotope Substitution in a Water-in-Oil Microemulsion: Quasi-elastic Light Scattering

Piero Baglioni and Luigi Dei

Department of Chemistry, University of Florence, V. G. Capponi 9, 50121 Florence, Italy

Cecilia M. C. Gambi*

Department of Physics, University of Florence, L. E. Fermi 2, 50125 Florence, Italy

Received: May 30, 1994; In Final Form: October 12, 1994[⊗]

Isotope substitution is currently used by several techniques such as small-angle neutron scattering (SANS), electron spin echo modulation (ESEM), and nuclear magnetic resonance (NMR), which are able to provide information at a molecular level. This substitution was found to produce changes in several physical processes (i.e., phase transitions, coexistence curves, critical phenomena, etc.). The effect of the isotope substitution and in particular the effect of perdeuteration of a component is not fully understood yet, and in some cases, contradictory results have been obtained. This paper reports a quasi-elastic light-scattering (QELS) study of water/oil microemulsions in which water, oil, and alcohol have been selectively deuterated. The results show that selectively deuterated microemulsions are similar to non-deuterated ones, in agreement with the fact that the phase diagram is not dramatically changed. The microemulsion droplets have a radius of about 100 Å, and the interdroplet interactions can be described by a hard-sphere repulsion potential and an attractive term due to Van der Waals interactions. The salinity has a similar role for both deuterated and non-deuterated microemulsions. Higher salinities favor higher curvatures. Changes in the hydrodynamic radius and in the second virial coefficient of the interdroplet interaction potential are found upon deuteration of different regions of the microemulsions.

Introduction

In several modern techniques such as small-angle neutron scattering (SANS), electron spin echo modulation (ESEM), and nuclear magnetic resonance (NMR), isotope substitution is used in order to improve the "contrast" between two different regions of a system, for example, water and hydrocarbon or hydrocarbons of different kinds or polymer and solvent, etc. Typical examples of systems studied with these techniques are micelles,[1-10] microemulsions,[11-19] vesicles,[17,20-22] polymeric solutions,[17,23,24] and biological compounds.[17,22]

The isotope substitution produces remarkable effects which have been discussed for micelles,[1-5] polymers in solutions,[24] and microemulsions.[11-13,16] In these dispersed systems, the origin and the cause of perturbation arising from the perdeuteration of a component are not yet well understood. In some water-in-oil microemulsions,[11] the stronger hydrogen bonding in H_2O than in D_2O is suggested to explain surface charge density changes. Structural studies have shown that in microemulsions different physical properties deriving from the perdeuteration of H_2O[12,13,16] or hydrocarbons[13,16] are not due to the changes in size and size distribution of the dispersed aggregates, but rather to the alteration of the aggregates interactions. We recently investigated, by using the ESEM technique, the interfacial region of Winsor microemulsions.[25,26] These microemulsions (composed of a toluene/brine ratio ~1 (w/w) and of sodium dodecyl sulfate and 1-butanol in the proportions of 4% and 2% (w/w total), respectively) exhibit a rich phase behavior simply by changing the brine salinity in the range 3%−10% (w/w). Oil-in-water (o/w), bicontinuous, and water-in-oil (w/o) microemulsions are shown at low, intermediate, and high sodium chloride content.[27] The o/w (I), the bicontinuous (III), and the w/o (II) microemulsions form in equilibrium with oily, oily and aqueous, and aqueous solutions, respectively. The composition of the droplet core is the same as that of the corresponding excess phase.[28,29] Therefore, oil-in-water droplets have a core composed of oil and some alcohol molecules, whereas water-in-oil droplets have a core composed of brine and some alcohol molecules. The droplet interfacial region is composed of alcohol and all the surfactant molecules (if we neglect the small amount of surfactant dispersed in the continuous phase); the continuous phase is composed of brine and alcohol for the o/w microemulsion and oil and alcohol for the w/o microemulsion. Hence, the alcohol parts between core, interface, and continuous phase (the alcohol content in the core and in the continuous phase is very low, few percents by weight, whereas the alcohol/surfactant mole ratio of the interface is about 1 or 2). A deeper insight on the interfacial composition of Winsor microemulsions was provided by ESEM, which gives information at a molecular level.[25,26] In this study, the components of the Winsor microemulsions were selectively deuterated and a shift of the phase transition boundaries was observed.[25] Similar shifts have been reported in other studies.[11-13,16] In order to clarify the effect of the isotope substitution on the structure of the w/o microemulsions, this paper reports a quasi-elastic light-scattering (QELS) study of selectively deuterated microemulsions, with the same molar composition of the non-deuterated microemulsions corresponding to 9% and 10% salinity.

Experimental Section

Materials. Toluene, 1-butanol, sodium dodecyl sulfate (SDS), and sodium chloride were Merck products. The water was obtained from a Millipore Milli-Q system. Deuterated 1-butanol-d_{10}, toluene-d_8, and D_2O (purity ≥ 99%) were from Aldrich. All the products were used without further purification. The samples were stabilized at $T = 22.0 \pm 0.1$ °C in a

[⊗] Abstract published in *Advance ACS Abstracts*, March 1, 1995.

0022-3654/95/2099-5035$09.00/0

TABLE 1 [a]

		A.DW	A.DO	A.DA	B.DW	B.DO	B.DA
$(a/b)_{gc}$	10^{-3} m/m	3.72 ± 0.04	3.25 ± 0.03	3.21 ± 0.03	3.95 ± 0.04	3.44 ± 0.035	3.47 ± 0.035
$(a/o)_d$	10^{-2} m/m	5.92 ± 0.04	5.81 ± 0.04	4.89 ± 0.03	5.57 ± 0.04	5.69 ± 0.04	5.12 ± 0.03
a/s	m/m	2.2 ± 0.2	2.3 ± 0.2	3.0 ± 0.28	2.3 ± 0.2	2.3 ± 0.2	2.7 ± 0.25
$(b/s)_m$	m/m	50 ± 1.6	52 ± 1.6	54 ± 1.6	60 ± 2	64 ± 2	65 ± 2
ϕ	cm^3/cm^3	0.151 ± 0.002	0.146 ± 0.002	0.154 ± 0.002	0.171 ± 0.002	0.165 ± 0.002	0.171 ± 0.002
ϕ_c	cm^3/cm^3	0.105 ± 0.003	0.099 ± 0.003	0.101 ± 0.003	0.123 ± 0.003	0.119 ± 0.003	0.121 ± 0.003
η	10^{-2} poise	0.583	0.618	0.584	0.583	0.618	0.584
R_H	Å	92 ± 2	84 ± 2	89 ± 2	107 ± 2	118 ± 8	122 ± 4
α		−2.9 ± 0.3	−2.9 ± 0.3	−4.0 ± 0.3	−4.2 ± 0.3	−4.9 ± 0.4	−5.1 ± 0.4
R_c	Å	81 ± 2	74 ± 2	77 ± 2	96 ± 2	106 ± 7	109 ± 3.6
Σ	$Å^2$	63 ± 3	65 ± 3	63 ± 3	64 ± 3	56 ± 5	55 ± 3

[a] Alcohol/brine ratio obtained by gas chromatographic analysis, $(a/b)_{gc}$, alcohol/oil ratio obtained by the dilution procedure, $(a/o)_d$, calculated alcohol/surfactant interfacial ratio, a/s, and brine/surfactant microemulsion ratio, $(b/s)_m$ (all in mole ratios); volume fraction of the dispersed phase, ϕ, and volume fraction of the core phase, ϕ_c; viscosity of the continuous phase, η; hydrodynamic radius of the droplets, R_H, and second virial coefficient, α, obtained from light-scattering analysis; calculated core radius, R_c, and area per polar head of the surfactant molecule, Σ. The errors reported are standard deviations, one half-width of the Gaussian distribution.

thermostated bath for more than 1 week until the equilibrium was attained. The phases were separated in a stabilized chamber at the same temperature as the bath, with the care necessary to obtain reproducible results, and then replaced in the same bath. No further phase separation was then observed. In this paper, samples A and B correspond to salinity values of 10% and 9% and DW, DO, and DA indicate samples with deuterated water, deuterated oil, and deuterated alcohol, respectively.

Methods. The study of microemulsion systems by dynamic light scattering is widely used since laser sources have been employed and digital correlators developed to directly measure the time-dependent autocorrelation function of the scattered light intensity which is related to the Brownian motion of the microemulsion droplets and makes it possible to determine the mutual diffusion coefficient of the droplets.[30-31] QELS experiments were carried out on a Brookhaven apparatus (BI 200SM with BI2030AT) by using a Coherent argon ion laser ($\lambda = 514$ nm) with a long-term power stability of ±0.5%. The scattered light intensity was detected by a EMI 9863B/350 photomultiplier. A calibration procedure was carried out on a diluted monodispersed suspension of polystyrene latex spheres (Serva, 0.06 μm). The data were analyzed using the cumulant technique. The autocorrelation function is expanded about an average line width Γ as a polynomial in the sample time with cumulants as parameters to be fitted.[32,33] The expansion is stopped to the second-moment result, and a weighted, least-squares technique is applied to the second-order polynomial to determine the constants and their standard deviations. The so-called average mutual diffusion coefficient D is related to Γ by the relation $D = \Gamma/K^2$, where $K = (4\pi n/\lambda)\sin(\theta/2)$ is the scattering wave vector, n the index of refraction of the sample, and θ the scattering angle. The deviation of the experimental curve from a single exponential decay is usually given by μ_2/Γ^2 (where μ_2 is the second moment of the distribution) and is called "degree of polydispersity".[33] The sample cells used in experiments were 5 mm diameter ultraprecision sealed glass cylindrical cells (Aldrich NMR, premium tubes). The index of refraction of the samples was measured by an Abbe refractometer (Atago 3T) with an accuracy better than 0.001. Viscosities of the continuous phases were measured by an Ubbelhode viscometer with an accuracy of 1%. All the measurements were performed at $T = 22 \pm 0.1$ °C.

Results and Discussion

Before dealing with the QELS results, we report the microemulsion composition study mainly performed by gas chromatographic analysis of the excess phases and dilution of the microemulsion samples. All the measurements were performed at the temperature of the QELS study. The alcohol/brine ratio of the excess aqueous phases, $(a/b)_{gc}$, measured by gas chromatographic analysis, is reported in Table 1. As already reported in the Introduction, this ratio corresponds to the alcohol/brine ratio of the microemulsion core. The alcohol/oil ratio of the continuous phase, $(a/o)_d$, was obtained, by following the dilution procedure,[34] by adding to the microemulsion sample a measured amount of oil and further titrating with alcohol to reobtain a monophasic sample. For all the samples studied, straight titration curves were found, as shown in Figure 1, at a dilution below 1/6. The $(a/o)_d$ ratios are reported in Table 1. For each sample the volume ratio (r) between the excess phase and the total was measured with a standard deviation $\sigma_r = 0.002$; the r values found are 0.360 cm^3/cm^3 for A samples and 0.348 cm^3/cm^3 for B samples. For each series (A and B), within the

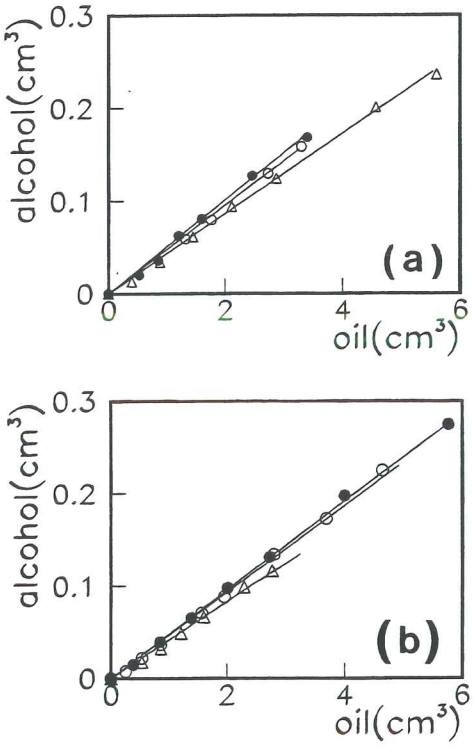

Figure 1. Titration curves for microemulsions of the A series (a) and B series (b). Symbols: full circles indicate samples with deuterated water, open circles samples with deuterated oil, and triangles samples with deuterated alcohol. Least-square fittings were performed on straight lines of equation $y = mx$, scaling the weight of the data points according to the accuracy (better at higher x values). The error bars (standard deviations) are smaller than the symbols used.

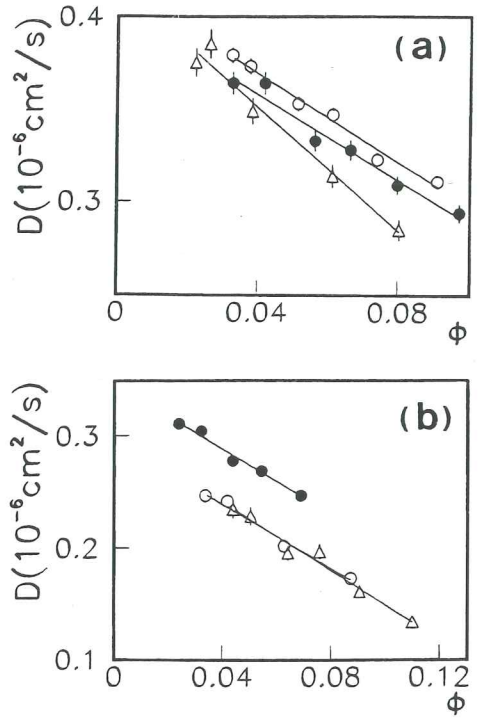

Figure 2. Mutual diffusion coefficient D as a function of the volume fraction of the dispersed phase, ϕ, for microemulsions of the A series (a) and B series (b). The symbols have the same meaning as those in Figure 1. The error bars are standard deviations.

accuracy of the measurements, no variation of the r value was detected for the deuteration of the components. Once the alcohol/brine ratio of the water core, the alcohol/oil ratio of the continuous phase, and the volume ratio of the excess phase to the total are known, the compositions of the core, of the interface, and of the continuous phase are obtained. To facilitate the discussion of the results, the interfacial alcohol/surfactant ratio, a/s, the microemulsion brine/surfactant ratio, $(b/s)_m$, the volume fraction of the dispersed phase, ϕ = (core + interface)/total, and the volume fraction of the core phase, ϕ_c = core/total are also reported, for each sample, in Table 1. The observation of titration straight lines (see Figure 1a,b) represents experimental evidence that the droplet radius remains constant upon dilution of the microemulsion up to 1/6.[27,35] In such a case, we can find a ϕ interval where the relation $D(\phi) = D_o(1 + \alpha\phi)$ applies;[36] D is the mutual diffusion coefficient of each sample, D_o is the self-diffusion coefficient extrapolated at infinite dilution, and α is a constant (virial coefficient) related to the interactions between droplets. The experimental mutual diffusion coefficient as a function of ϕ is reported in Figure 2a for diluted samples of the A series and in Figure 2b for diluted samples of the B series. In the studied angular range (20°–160°), $D(\theta)$ is a constant within ±1% for all the samples of Figure 2 and the polydispersity value, as obtained by the second moment of the cumulant distribution, is 5%–8%. The samples of Figure 1a,b have volume fractions of the dispersed phase in the range 0.14–0.02 for the A series and 0.16–0.02 for the B series; samples with ϕ values larger than those reported in Figure 2 exhibit an angular dependence of D which is typical of multiple scattering.[37] Once D_o and α are known, the hydrodynamic radius of the droplets (R_H) can be obtained from the Stokes–Einstein relation[31] $D_o = k_BT/(6\pi\eta R_H)$ (k_B is the Boltzmann constant, T the absolute temperature, and η the viscosity of the continuous phase). D_o and α were calculated by linear regression of the experimental points of Figure 2, and the R_H values were determined from the Stokes–Einstein relation. R_H and α with their errors are reported in Table 1. No QELS signal was shown by the excess phases of the A and B samples, supporting that no structural aggregates are present. In Table 1, the core radius of the droplets, R_c, as obtained by the relationship $(R_c/R_H)^3 = \phi_c/\phi$,[38,39] and the area per polar head of the surfactant molecule $\Sigma = 3\phi_c/n_sR_c$,[39] where n_s is the number of surfactant molecules per unit volume of the microemulsion, are also reported. R_H, R_c, and Σ are reasonable estimates of the droplet radius, of the core radius, and of the interfacial area per polar head, under the assumption that the microemulsion is composed of monodispersed, spherical, undeformable droplets.

The results obtained for the deuterated w/o microemulsion are similar to those of the non-deuterated microemulsion,[27] in agreement with the fact that the phase diagram does not change dramatically upon deuteration. In fact, the microemulsion droplets have radii of about 100 Å and the interdroplet interactions can be described by a hard-sphere repulsion potential and an attractive term due to Van der Waals interactions, according to Vrij et al.[40–42] Furthermore, the salinity plays for the deuterated microemulsion a role similar to that of the non-deuterated samples.[27] At higher salinity (A series), the screening of the electrostatic effect of the surfactant molecules favors higher curvatures; therefore, the hydrodynamic radius of the A series is lower than that of the B series.

In the limit of the experimental errors, the interfacial thickness $t = R_H - R_c$ is almost constant and about 11 Å (with ±10% accuracy) for all the samples, regardless of the deuteration of alcohol, which belongs to the interfacial layer, and the deuteration of the neighboring water or oil molecules. The thickness value agrees with that of the non-deuterated samples. Note that sodium dodecyl sulfate, with an elongated chain of 21 Å, and n-butanol form a layer of about 11 Å thickness.[14,35,38] The surfactant may have both an extended and a folded conformation, as already found for the non-deuterated system.

QELS analysis indicates that structural changes are related to the deuteration and to the deuterium location of the microemulsion components. We observed different structural changes for the two series. We will discuss the results obtained for the differently deuterated regions of the A and B microemulsion in relation to the deuterated water sample.

A Series. By deuterating the oil instead of water, the interfacial alcohol to surfactant ratio a/s and the brine to surfactant ratio $(b/s)_m$ of the microemulsion droplet are unchanged, in the limit of the experimental errors. Moreover, the alcohol content is lowered both in the core and in the continuous phase, as deduced by the decrease of the $(a/b)_{gc}$ and $(a/o)_d$ ratios. The volume fractions of the dispersed phase and that of the core phase (ϕ and ϕ_c) are slightly lowered. The hydrodynamic radius and the core radius, R_H and R_c, are lowered whereas the area per polar head Σ is constant. The number of droplets for unit volume, which can be easily estimated since it is proportional to ϕ/R_c^3, increases. Therefore the deuteration of oil instead of water produces a system composed of a slightly higher number density of smaller droplets. As the second virial coefficient α is identical in deuterated water and deuterated oil samples, the interdroplets interactions are also identical. These results clearly show that the isotope substitution of hydrogen with deuterium, outside the droplet, does not affect the interfacial composition. It is known[24,43] that the carbon–deuterium bond has a smaller length and a lower polarizability than the carbon–hydrogen bond. The lower polarizability of the deuterated in relation to the hydrogenated bond has been also deduced by surface tension measurements on a series of perdeuterated hydrocarbons, including toluene-d_8.[44] Furthermore, recent studies[43,45] on binary n-alkane mixtures (one hydrogenated and the

other deuterated) show that CD_2 groups have a lower volume than CH_2 groups and that the change in the volume difference, which occurs when hydrogen and deuterium are interchanged, is a significant fraction of the actual volume difference between the two chains. It follows that deuterated oil penetrates the interface more than protonated oil, favoring an increase in the droplet curvature.

The deuteration of alcohol instead of water produces a decrease of alcohol both in the core, $(a/b)_{gc}$, and in the continuous phase, $(a/o)_d$, and an increase of alcohol at the interface, a/s (see Table 1). However, the microemulsion brine/surfactant ratios ϕ and ϕ_c are very similar. The hydrodynamic radius, the core radius, the area per polar head of the surfactant molecule, and the number of droplets for unit volume are also very similar. On the contrary, the second virial coefficient is lower, indicating that the interdroplet interactions are more attractive. A deeper insight on the role of deuteration in the microemulsions studied can be obtained by using a model for the calculation of the mean-field interparticle potential for water-in-oil microemulsions.[46,47] In this model the microemulsion droplet is composed of two parts, one impenetrable, formed by an aqueous core and an interfacial layer up to the end of the alcohol chain, and the other penetrable, formed by a layer extending from the end of the alcohol chain to the end of the surfactant chain. The radius of the whole aggregate (hydrodynamic radius) is larger than the hard-sphere radius, that is, the impenetrable part. According to Vrij,[40-42] the total interparticle potential is composed of the repulsive hard-sphere potential and of the attractive part. The variation of the internal energy of the overlapped region, before and after penetration of neighboring droplets, has been calculated in detail.[46,47] During overlapping, two steps may be considered. (1) When overlapping is not too large, there is only an exchange of solvent molecules dissolved at the interface by the chain segments of surfactant molecules. (2) When there is a larger overlap, surfactant chains are confined in a smaller volume due to the presence of the two hard alcohol layers. This removes the molecules of the continuous phase, leading to an increase of the surfactant CH_2 and CH_3 group volumes. Interaction energies of nonoverlapping volumes lead to negligible values in relation to the overlap contribution, which give attractive interactions. Entropic contributions which are repulsive are induced by the constraints applied to surfactant chains during large overlapping. This contribution is also negligible. Light-scattering results, interpreted according to this model, can provide detailed information on the structure of the microemulsion system.[47,48] The main features obtained are (i) the hydrodynamic radius increases as a function of the water to surfactant ratio, and it is independent of the alcohol length; (ii) the second virial coefficient, however, strongly depends on the alcohol, and the increase of the alcohol chain length decreases the attractive interactions due to the decrease of the volume of the penetrable part; and (iii) the volumes of the CH_2 and CH_3 groups depend only on the chemical nature of the oil (*n*-alkane) and of the surfactant. The parameters reported in Table 1 have been calculated by considering all the surfactant molecules into the interfacial region regardless of the molecule location in the hard inner layer (thickness of about 11 Å) and in the outer layer. No oil amount has been introduced in the calculation of ϕ and ϕ_c. The oil in our microemulsion system is toluene and behaves as an n-alkane of similar molecular weight.[47] The salt is inside the water droplet, and we can reasonably assume that, for a given series, the differences between deuterated oil and deuterated and alcohol samples, in relation to deuterated water sample, are not affected by salt. *n*-Butanol is shorter than pentanol; therefore, we expect a thinner layer of the inner part of the interface in relation to that of other alcohols. In fact, it has been demonstrated[47,48] that changes in the alcohol chain length (from pentanol to heptanol) do affect only the length of the penetrable part of the interface.

Table 1 shows that deuteration of alcohol increases the ratio of interfacial alcohol to surfactant. This increase does not affect the area per polar head of the surfactant molecule, while it is associated to an increase in the second virial coefficient magnitude. This behavior can be explained by considering two effects. One is related to the smaller volume of the alcohol methyl and methylene deuterated groups, which facilitates the increase of the total amount of alcohol at the interface, and the other is related to the location of the alcohol molecule at the interface. The increase of the second virial coefficient magnitude suggests that the volume of the penetrable part of the interface is increased upon alcohol deuteration. This can be accomplished by considering the smaller volume of the deuterated alcohol chain and by considering that alcohol molecules move toward the water side of the interface as demonstrated by ESEM results.[25] In fact, the normalized deuterium modulation depth of the deuterated alcohol sample with the highest salinity value (the salinity of the A series) shows a lower value than that of the deuterated water sample.

B Series. By deuterating the oil instead of water, the interfacial alcohol to surfactant ratio a/s is identical and the brine to surfactant ratio $(b/s)_m$ of the microemulsion droplet is slightly higher. The alcohol content is lowered in the core ($(a/b)_{gc}$) and slightly increased in the continuous phase ($(a/o)_d$). ϕ and ϕ_c are slightly decreased. The deuteration of alcohol instead of water produces an effect similar to that of deuterated oil on the alcohol to brine ratio in the core and on the brine to surfactant droplet ratio. On the contrary, the alcohol content is decreased in the continuous phase and increased at the interface; ϕ and ϕ_c are unchanged, in the limit of the experimental errors. The hydrodynamic radius and the core radius (R_H and R_c) as well as the second virial coefficient magnitude increase when oil is deuterated. This increase is greater for deuterated alcohol. The area per polar head, Σ, decreases to a lower value in a similar way, for both deuterated oil and alcohol. The deuteration of oil or alcohol produces a lower number density of larger droplets. The QELS results of deuterated oil sample have a lower accuracy, and therefore, the interpretation of the results could be somewhat ambiguous.

We compare now the results of the deuterated water samples A and B. The interfacial alcohol to surfactant ratio and the area per polar head have the same value, in the limit of the experimental accuracy. The alcohol to brine ratio is higher for sample B, whereas the alcohol to oil ratio is lower for sample B. The higher brine to surfactant ratio of sample B implies a higher hydrodynamic radius, as experimentally observed. The second virial coefficient magnitude is higher for sample B, indicating higher attractive interdroplet interactions.

Comparing the deuterated oil samples A and B, the greater differences are observed for the hydrodynamic radius, the area per polar head, and the second virial coefficient magnitude. The analysis of ESEM data[25,26] can be used to clarify the interpretation. The normalized deuterium modulation depth arising from the deuterated oil of sample B is lower than that of sample A. This supports that oil penetrates deeper into the interfacial film in sample A, which has higher curvature.

The composition differences between samples A and B with deuterated alcohol are weak. The brine to surfactant ratio variation is compatible with the curvature change. The interfacial area per polar head is strongly decreased for sample B.

This clearly shows that the change of curvature implies a reorganization of the molecules at the interface. Therefore, the sample B with deuterated alcohol, the increase of the volume of the penetrable part of the interface is related to the shift of the alcohol molecules toward the water side.[25,26] This effect is less important in sample B than in A. Moreover, the higher the second virial coefficient magnitudes of deuterated water, deuterated oil, and deuterated alcohol of samples B, seem mainly related to the curvature change.

Conclusion

In summary, for the A series, the salinity value is high enough to screen the electrical charge of the surfactant molecule and the selective deuteration of the components does not change the geometry of the interfacial region, i.e. area per polar head and thickness are constant. Deuterated oil produces a higher curvature likely because it penetrates the interface more than protonated oil, while deuterated alcohol produces stronger attractive interactions mainly due to the increase of the volume of the penetrable part of the interface, which is due to a shift of the alcohol molecules toward the water side of the interface.

For the B series, the interfacial thickness is about the same as that of the A series and remains constant upon the components' deuteration. The interfacial area per polar head of the deuterated water sample is the same for both series. This fact indicates that for w/o microemulsions the deuteration of water does not significantly affect the interfacial microemulsion structure. Both deuterated oil and alcohol produce different trends in structural changes in the B series in relation to the A series. Differences are mainly due to the decreased screening of the electrical charge, which makes possible a variation of the interfacial molecular packing. This makes also possible the formation of larger droplets.

This picture is consistent with previous findings obtained by electron spin echo modulation analysis of the microemulsion interfacial layer, that provided information at the molecular level on the local interfacial layer composition.[25,26] In fact, ESEM results show the penetration of oil inside the interface and the alcohol shift toward the water side, which are higher for greater curvature. This is in agreement with the change of the second virial coefficient as a function of the microemulsion component deuteration.

Acknowledgment. The authors wish to thank Dr. Gloria Menchi (Department of Organic Chemistry "U. Schiff") for the gas chromatographic measurements. Thanks are also due to the National Council for Research (CNR) and the Ministery of University and Scientific and Technical Research (MURST) of Italy for financial support. This research is also supported in part by European Community Grant No. ERBCHRXCT 920007.

References and Notes

(1) Chang, N. J.; Kaler, E. W. *J. Phys. Chem.* **1985**, *89*, 2996–3000.
(2) Degiorgio, V.; Piazza, R.; Corti, M.; Minero, C. *J. Chem. Phys.* **1985**, *82* (2), 1025–1031.
(3) Binana-Limbelé, W.; Zana, R. *J. Colloid Interface Sci.* **1988**, *121* (1), 81–84.
(4) Candau, S.; Hirsch, E.; Zana, R. *J. Colloid Interface Sci.* **1982**, *88* (2), 428–436.
(5) Calfors, J.; Stilbs, P. *J. Colloid Interface Sci.* **1985**, *104* (2), 489–499.
(6) Lindman, B.; Stilbs, P. *Physics of Amphiphiles: Micelles, Vesicles and Microemulsions*; Società Italiana di Fisica: Bologna, Italy, 1985; pp 94–121.
(7) Baglioni, P.; Dei, L.; Kevan, L.; Rivara-Minten, E. In *Mixed Surfactant Systems*; Holland, P. M., Rubingh, D. N., ACS Symposium Series 501; American Chemical Society: Washington, DC, 1992; Chapter 10, pp 180–193.
(8) Baglioni, P.; Bongiovanni, R.; Rivara-Minten, E.; Kevan, L. *J. Phys. Chem.* **1989**, *93*, 5574–5578.
(9) Baglioni, P.; Ferroni, E.; Kevan, L. *J. Phys. Chem.* **1990**, *94*, 4296–4298.
(10) Baglioni, P.; Dei, L.; Rivara-Minten, E.; Kevan, L. *J. Am. Chem. Soc.* **1993**, *115*, 4286.
(11) Chou, S. I.; Shah, D. O. *J. Colloid Interface Sci.* **1981**, *80*, 49–57; *J. Phys. Chem.* **1981**, *85*, 1480–1485.
(12) Chang, N. J.; Kaler, E. *Langmuir* **1986**, *2*, 184–190.
(13) Huang, J. S.; Sung, J.; Wu, X.-L. *J. Colloid Interface Sci.* **1989**, *132* (1), 34–42.
(14) Auvray, L.; Cotton, J. P.; Ober, R.; Taupin, C. *J. Phys.* **1984**, *45*, 913–928; *J. Phys. Chem.* **1984**, *88*, 4586–4589; *Physica* **1986**, *136B*, 281–283.
(15) Guéring, P.; Lindman, B. *Langmuir* **1985**, *1*, 464–468.
(16) Tabony, J.; Drifford, M.; De Geyer, A. *Chem. Phys. Lett.* **1983**, *96* (1), 119–125.
(17) *Scattering Techniques Applied to Supramolecular and Nonequilibrium Systems*; Chen, S.-H., Chu, B., Nossal, R., Eds.; Nato Advanced Study Institutes Series, Series B: Physics B73; Plenum Press: New York, 1981.
(18) Baglioni, P.; Nakamura, H.; Kevan, L. *J. Phys. Chem.* **1991**, *95*, 3856–3859.
(19) Stilbs, P.; Lindman, B. *Prog. Colloid Polym. Sci.* **1984**, *69*, 39–47.
(20) Kevan, L.; Baglioni, P. *Pure Appl. Chem.* **1990**, *62*, 275–280.
(21) Sakaguchi, M.; Baglioni, P.; Kevan, L. *J. Phys. Chem.* **1992**, *96*, 2772–2776.
(22) Glatter, O. *Prog. Colloid Polym. Sci.* **1991**, *84*, 46–54.
(23) Bates, F. S.; Wiltzins, P. *J. Chem. Phys.* **1989**, *91* (5), 3258–3275.
(24) Jones, R. A. L.; Norton, L. J.; Kramer, E. J.; Bates, F. S.; Wiltzins, P. *Phys. Rev. Lett.* **1991**, *66* (10), 1326–1329.
(25) Baglioni, P.; Gambi, C. M. C.; Goldfarb, D. *J. Phys. Chem.* **1991**, *95*, 2577–2583.
(26) Baglioni, P.; Gambi, C. M. C.; Goldfarb, D. *Prog. Colloid Polym. Sci.* **1991**, *84*, 133–138.
(27) Cazabat, A. M.; Langevin, D.; Meunier, J.; Pouchelon, A. *Adv. Colloid Interface Sci.* **1982**, *16*, 175–199.
(28) Biais, J.; Bothorel, P.; Clin, B.; Lalanne, P. *J. Dispersion Sci. Technol.* **1981**, *2* (1), 67–95.
(29) Biais, J.; Barthe, M.; Clin, B.; Lalanne, P. *J. Colloid Interface Sci.* **1984**, *102* (2), 361–369.
(30) Berne, B. J.; Pecora, R. *Dynamic Light Scattering*; Wiley: New York, 1976.
(31) Pecora, R. In *Dynamic Light Scattering: Application of Photon Correlation Spectroscopy*; Plenum: New York and London, 1985.
(32) Koppel, D. E. *J. Chem. Phys.* **1972**, *57* (11), 4814–4820.
(33) Brown, J. C.; Pusey, P. N.; Dietz, R. *J. Chem. Phys.* **1975**, *62* (3), 1136–1144.
(34) Graciaa, A.; Lachaise, J.; Martinez, A.; Bourrel, M.; Chambu, C. *C. R. Acad. Sci., Ser. B* **1976**, *282*, 547–550.
(35) Brouwer, W. M.; Nieuwenhuis, E. A.; Kops-Werkhoven, M. M. *J. Colloid Interface Sci.* **1983**, *92* (1), 57–65.
(36) Felderhof, B. U. *J. Phys. A* **1978**, *11*, 929–937.
(37) Siano, D. B.; Berne, B.; Flynn, G. W. *J. Colloid Interface Sci.* **1978**, *63* (2), 282–289.
(38) Cazabat, A. M.; Langevin, D. *J. Chem. Phys.* **1981**, *74*, 3148–3158.
(39) De Gennes, P. G.; Taupin, C. *J. Phys. Chem.* **1982**, *86*, 2294–2304.
(40) Caljé, A. A.; Agterof, W. G. M.; Vrij, A. In *Micellization Solubilization and Microemulsions*; Mittal, K. L., Ed.; Academic Press: New York, pp 779–790.
(41) Agterof, W. G. M.; Van Zormern, J. A. J.; Vrij, A. *Chem. Phys. Lett.* **1976**, *43* (2), 363–367.
(42) Vrij, A.; Nieuwenhuis, E. A.; Fijnaut, H. M.; Agterof, W. G. *Faraday Discuss. Chem. Soc.* **1978**, *65*, 101–113.
(43) Dorset, D. L.; Strauss, H. L.; Snyder, R. G. *J. Phys. Chem.* **1991**, *95*, 938–940.
(44) Gaines, G. L., Jr.; Le Grand, D. G. *Colloid Surf. A* **1994**, *82*, 299–300.
(45) Snyder, R. G.; Srivatsavoy, V. J. P.; Cates, D. A.; Strauss, H. L.; White, J. W.; Dorset, D. L. *J. Phys. Chem.* **1994**, *98*, 674–684.
(46) Lemaire, B.; Bothorel, P.; Roux, D. *J. Phys. Chem.* **1983**, *87*, 1023–1028.
(47) Roux, D. Université de Bordeaux I Thesis, 1984.
(48) Brunetti, S.; Roux, D.; Bellocq, A. M.; Fourche, G.; Bothorel, P. *J. Phys. Chem.* **1983**, *87*, 1023–1028.

JP9413861